A twist grain boundary phase with a local antiferroelectric structure

2000 J. Phys.: Condens. Matter 12 8577

(http://iopscience.iop.org/0953-8984/12/40/303)

J. Phys.: Condens. Matter **12** (2000) 8577–8593. Printed in the UK PII: S0953-8984(00)13138-8

A twist grain boundary phase with a local antiferroelectric structure

A S Petrenko†, M Hird†, R A Lewis†, J G Meier‡, J C Jones§ and J W Goodby†‖

† Department of Chemistry, University of Hull, Hull HU6 7RX, UK
‡ Department of Microelectronics and Nanoscience, Chalmers University of Technology, SE-41296 Gothenburg, Sweden
§ DERA, St Andrews Road, Great Malvern, Worcestershire WR14 3PS, UK

Received 7 April 2000, in final form 9 May 2000

Abstract. (S)-1-methylheptyl 2-[4-(4-dodecyloxybenzoyloxy)phenyl]pyrimidine-5-carboxylate and its racemic modification were synthesized. Through miscibility studies, investigations of defect textures, differential scanning calorimetry and electrical field studies, we conclude that this material exhibits an antiferroelectric twist grain boundary $TGBC^{*}_{A}$ analogue of the Abrikosov flux phase found in superconductors. This outcome represents the addition of a new frustrated state of matter to the family of twist grain boundary phases. This novel phase was found to exist between the isotropic liquid and the antiferroelectric smectic C^{*} phase.

1. Introduction

The prediction [1, 2] and discovery [3, 4] of the twist grain boundary (TGB) smectic A^{*} phase led to the unification of phase transitions in liquid crystals with those found for superconductors. Apart from the unification of these two dissimilar physical phenomena, TGB phases have been found to be ubiquitous in the field of self-organizing systems with such frustrated phases mediating phase transitions from either the isotropic liquid or the chiral nematic phase to the smectic state [5–7].

Over the past ten years a number of TGB phases have been identified and characterized. Generally the structures of TGB phases have been found to be based on the structures of the smectic phases that they either replace or which they form upon cooling. Frustrated equivalents of the smectic A^{*} and C^{*} phases have been found, with both having variants that are dependent on the commensurability or incommensurability of the number of sheets of screw dislocations with respect to the pitch length of the phase [8, 9]. For the TGBC modification a number of subphases have been discovered which are dependent on (i) the presence ($TGBC^{*}$) or expulsion (TGBC) of the local heli-axis of the smectic C^{*} phase which is oriented perpendicular to the layers of molecules and to the heli-axis of the TGB phase, (ii) the inversion of the handedness of the helix in the TGBC phase as a function of temperature [10] and (iii) the formation of a 2D modulated structure with respect to the tilt [11].

It is interesting to note that the first TGB phases to be found were discovered in the (S or R)-1-methylheptyl 4′-(4-alkoxyphenylpropioloyloxy)biphenyl-4-carboxylates, **I** [3, 4]. In fact it appears that TGB phases often occur in conjunction with other frustrated phases such as blue

‖ Corresponding author.

0953-8984/00/408577+17$30.00

phases, SmC^*_α, SmC^*_β, SmC^*_γ, SmC^*_{AF}, and SmC^*_A. Although through the medium of chirality the unification of superconductors with liquid crystals appears to have been achieved [1, 2], it also seems that chirality dependent frustrations unify a variety of structures of mesophases that exhibit nonlinear physical properties [12].

In this present investigation we report on the liquid crystal properties of a related compound (S)-1-methylheptyl 2-[4-(4-dodecyloxybenzoyloxy)phenyl]pyrimidine-5-carboxylate, **II**, and its racemic modification. Through miscibility studies, investigations of defect textures, differential scanning calorimetry and electrical field studies, we conclude that this material exhibits an antiferroelectric $TGBC^*_A$ mesophase.

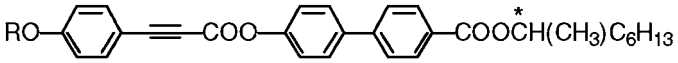

I

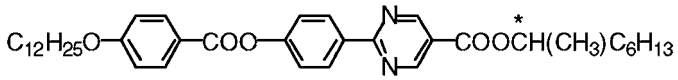

II

2. Experimental methods

2.1. General synthetic procedures

The synthetic route to (S)-1-methylheptyl 2-[4-(4-dodecyloxybenzoyloxy)phenyl] pyrimidine-5-carboxylate, **II**, is shown in scheme 1. The racemic modification was prepared in exactly the same way as the (S)-enantiomer except that (R)-2-octanol was replaced with racemic 2-octanol. The key to the synthesis is the preparation of 5-bromo-2-iodopyrimidine, **6** [13], which can be selectively coupled to a benzyloxy protected phenylboronic acid, **3**. 5-Bromo-2-iodopyrimidine was prepared by bromination of 2-hydroxypyrimidine followed by chlorination with phosphorus oxychloride to yield 5-bromo-2-chloropyrimidine, **5**. It should be noted that in this procedure the reaction mixture was slowly poured onto ice with extreme care and the product was isolated by extraction into ether. Compound **5** was subsequently treated with hydriodic acid to give **6** in good yield.

4-Benzyloxyphenylboronic acid, **3**, was prepared from 4-bromophenol, **1**, by treatment with benzyl bromide in the presence of potassium carbonate to yield 4-benzyloxyphenyl bromide **2**. Compound **2** was first treated with *n*-butyllithium followed by trimethyl borate to give the boronic acid **3**. A Suzuki coupling procedure [14], in the presence of Pd(0) was used to couple compounds **3** and **6** to give 2-(4′-benzyloxyphenyl)-5-bromopyrimidine, **7**. The terminal bromine in **7** was converted to an acid by reaction with *n*-butyllithium followed by carbonation with solid carbon dioxide to give **8**. Compound **8** was esterified with (R)-2-octanol (or (±)-2-octanol to yield the racemic modification) in the presence of diethyl azodicarboxylate (DEAD) and triphenylphosphine [15] to give (S)-1-methylheptyl 2-(4-benzyloxyphenyl)pyrimidine-5-carboxylate, **9**. This material was deprotected by hydrogenolysis over palladium on charcoal (5%) and then esterified with 4-dodecyloxybenzoic acid, **11**, to give the final product **II**.

2.2. Characterization of materials

Phase identifications and determination of phase transition temperatures were carried out together by thermal polarized light microscopy. Homeotropic sample preparations suitable for

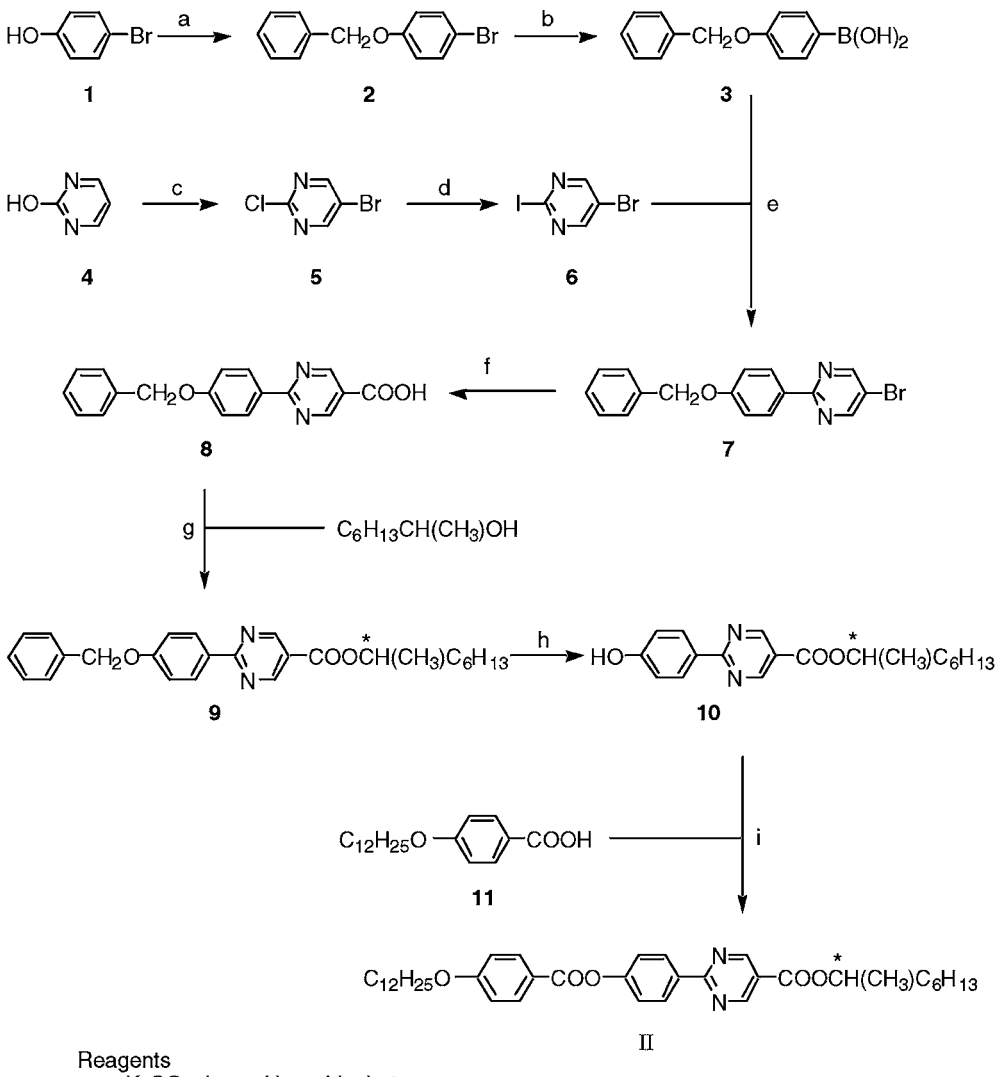

Reagents
a ... K_2CO_3, benzyl bromide, butanone
b ... (i) *n*-butyllithium, THF, -70 °C; (ii) $B(OMe)_3$
c ... (i) bromine; (ii) $POCl_3$
d ... HI, -5 °C
e ... (i) n-butyllithium, -100 °C; (ii)1,2-dimethoxyethane, $Pd(PPh_3)_4$, , 2M Na_2CO_3
f ... (i) n-butyllithium, THF, -100 °C; (ii) CO_2; (iii) HCl
g ... DEAD, PPh_3, THF
h ... H_2, Pd/C, ethyl acetate
i ... DCC, DMAP, DCM

Scheme 1.

phase characterization were prepared by using cleaned glass microscope slides (washed with water, acetone, water, concentrated nitric acid, water and dry acetone), whereas homogeneous defect textures were obtained by not using specially cleaned slides. Differential scanning calorimetry was performed at scan rates of 2 and 10 °C min^{-1} and the results obtained were standardized relative to indium (measured onset 156.7 °C, ΔH 28.5 J g^{-1}, literature value [16] 156.6 °C, ΔH28.45 J g^{-1}).

Table 1. The transition temperatures (°C) and the associated enthalpies of transition [ΔH kJ g^{-1}] for (S)-1-methylheptyl 2-[4-(4-dodecyloxybenzoyloxy)phenyl]pyrimidine-5-carboxylate **II**, and its racemic modification. * denotes the enthalpies that were too small to be evaluated.

Chiral compound **II** Iso-TGBC$^*_A$	TGBC$^*_A$–SmC$^*_A$	SmC$^*_A$–cryst	mp
93	91.6	68.3	86.4
[−0.87]	[−0.22]	[−28.8]	

Racemic modification

I–SmA	SmA–SmC	SmC–SmC$_{alt}$	SmC$_{alt}$–cryst	mp
96	90.5	89.2	43.6	72.6
[−9.12]	[−]*	[−]*	[−34.8]	[75.6]

Electrooptic measurements were carried out using homogeneously aligned cells (Linkam) which were constructed from electrically conducting indium tin oxide (ITO) coated glass, treated with antiparallel-buffed polyimide (PI) coated layers so as to give sites for planar, homogeneous growth of the liquid-crystalline phase. The cell gap ($\sim$5 μm) maintained by glass spacers was verified by UV–VIS interferometry. The effective electrode areas of the cells used were 0.9 cm^2. The cells were filled by capillary action at atmospheric pressure, with the liquid-crystalline materials in the isotropic liquid state. Good alignment was achieved by cooling slowly ($<$0.1 °C min^{-1}) from the isotropic liquid into the required liquid crystalline phase while applying an electric field (square wave form, $V_{rms} = \pm 20$ V μm^{-1} and 200 Hz). Typically, spontaneous polarization values were measured by the triangular wave method. The triangular waveform for the electric field was generated by a Hewlett Packard 33120A 15 MHz function generator with a maximum amplitude of $\pm$10 V and a 32 $\pm$ 0.2 ns rise time. The output signal was amplified by a fixed gain ($\times$50) amplifier with a maximum amplitude of $\pm$175 V, 16.5 $\pm$ 0.3 ms rise time and 1 kHz waveform capability. A triangular voltage with $\pm$20 V μm^{-1} at 20 Hz was applied to the cell. An optical polarizing microscope was used for observing textural changes during the measurements. The current was measured by detecting the voltage change across a resistor of 100 kΩ, which was sufficiently small compared with the impedance of the cell connected in series, and amplified by the means of a variable gain operational amplifier with an input impedance $\gg$100 kΩ, therefore the current loss for the measurement was negligible.

The dielectric measurements were carried out in a cell constructed from ITO-conducting glass with a cell spacing of 50 μm and for which the inner surfaces had been coated with polyimide and anti-parallel buffed to promote homogeneous alignment of the liquid crystal. By applying a DC electric field of 10 V μm^{-1}, $f = 20$ Hz, with the material in its SmC$^*_A$ phase good planar alignment over a period of 10 h was achieved.

3. Results

3.1. Transition temperatures

The transition temperatures, and the associated enthalpies for each phase transition, for (S)-1-methylheptyl2-[4-(4-dodecyloxybenzoyloxy)phenyl]pyrimidine-5-carboxylate **II**, and its racemic modification, were determined by thermal polarized microscopy and differential scanning calorimetry, and are given together in table 1.

Figure 1. The defect texture of an uncovered droplet of the TGB phase supported on glass (× 100).

Firstly it should noted that the purities of the materials have been evaluated and found to be better than 99.5%. Therefore it should be emphasized that differences in transition temperatures between the enantiomer and its racemate are real, as are differences in phase sequences and phase types. Thus the differences are associated with the effects of chirality on the system. For example, the isotropization temperature for the racemate is higher than that for the enantiomer, whereas the transition to a tilted smectic phase is lower. Furthermore, the racemate and the enantiomer do not exhibit the same number of liquid crystal phases or the same phase sequences, but nevertheless the racemate exhibits smectic phases on cooling from the isotropic liquid and therefore it is highly unlikely that the chiral variant would exhibit a chiral nematic phase. Thus the high temperature phase of the enantiomer is expected to be smectic.

3.2. Defect textures

Homogenous, homeotropic, uncovered droplets, and free-standing film specimens of the chiral compound, **II**, were examined by thermal polarized light microscopy. The phase first formed from the isotropic liquid was irridescent and clearly helical. The phase did not exhibit either a focal conic, platelet or *schlieren* defect texture, and was not typical of a TGBA or TGBC phase. Figure 1 shows an uncovered film of the phase supported on cleaned glass. An apparent *schlieren* texture is observed, but on closer examination this texture shows some features associated with a focal conic pattern. At lower temperatures the transition to and from the smectic C_A^* phase was characterized with the formation of filaments typical of a TGB phase, see figure 2 [17].

A Grandjean planar texture, typical of a helical phase was obtained in a homogeneously aligned cell with a $\sim$5 μm spacing that had been antiparallel buffed, see figure 3. The platelet areas are associated with domains that have differing numbers of twists of the helical macrostructure associated with them. The fact that the heli-axis is normal to the glass substrates of the cell indicate that the twist is in the direction of the planes of the layers, i.e. typical of a TGB phase.

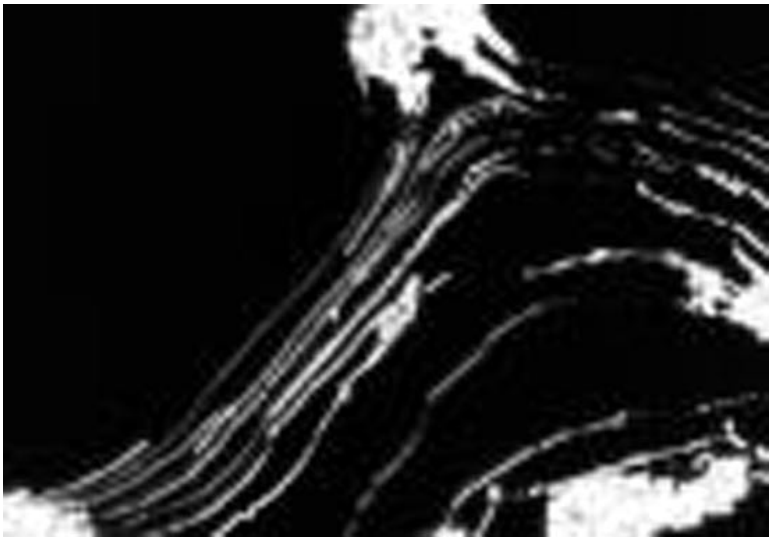

Figure 2. The filament texture of the TGB phase at the transition to the antiferroelectric phase ($\times$ 100).

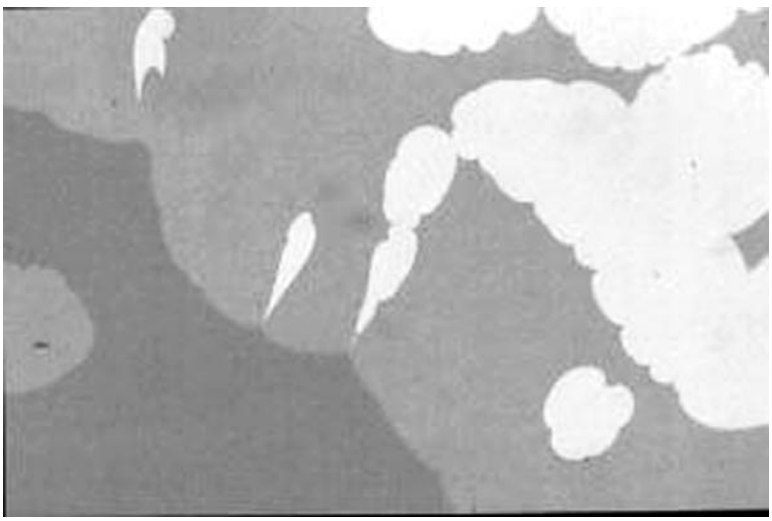

Figure 3. The Grandjean texture of the TGB phase in an aligned cell ($\times$ 100).

The presence of filaments and a heli-axis in the plane of the layers confirm that the phase formed first on cooling the isotropic liquid of the racemate is a twist grain boundary phase; however, the lack of a characteristic texture suggested that the phase was not of the type characterized so far.

Figure 4 shows a transition from the Grandjean texture of the TGB phase to the focal conic texture of the antiferroelectric smectic C_A^* phase. The formation of a homogeneous focal conic texture from a planar Grandjean texture indicates movement of the optic axis through 90° and confirms that the heli-axis is in the planes of the layers in the TGB phase. Figure 5 shows the fully developed focal conic texture of the antiferroelectric smectic C_A^* phase.

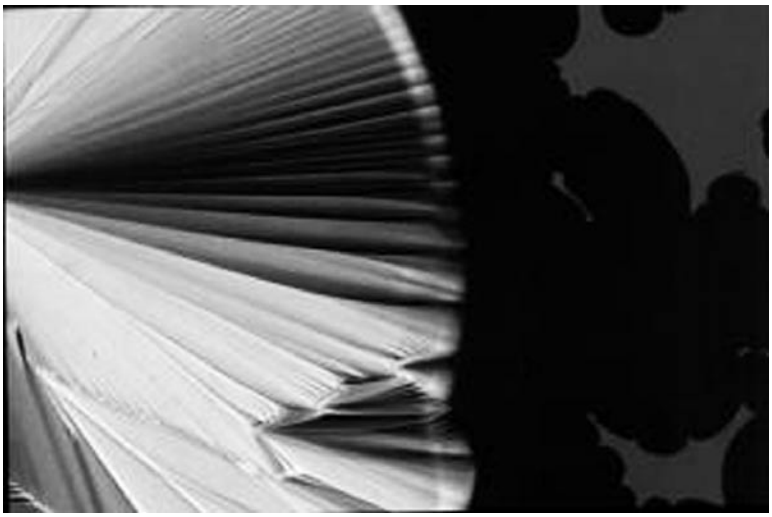

Figure 4. The transition from the Grandjean plane texture of the TGB phase to the focal conic texture of the antiferroelectric phase in an aligned cell ($\times$ 100).

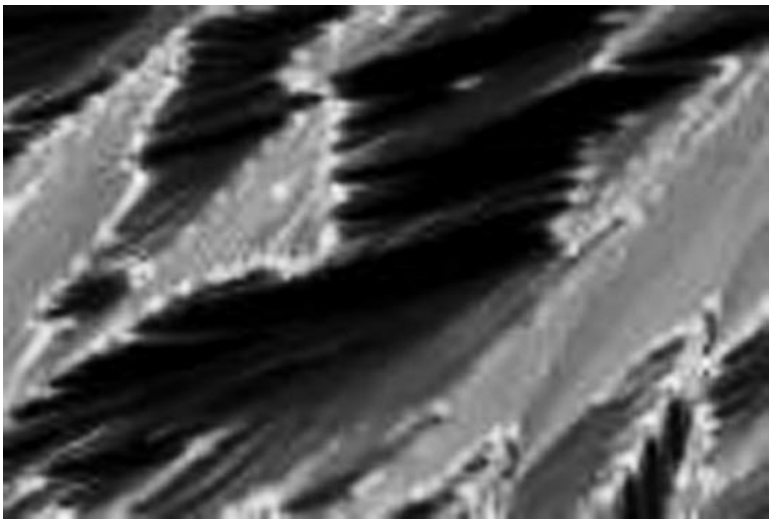

Figure 5. The focal conic texture of the antiferroelectric smectic C* phase in an aligned cell ($\times$ 100).

Comparing the results obtained for the racemic modification with those for the (S)-enantiomer yields some interesting and contrasting observations. The mesophase formed first on cooling the isotropic liquid of the racemic modification exhibits a focal-conic texture that is characterized by its elliptical and hyperbolic lines of optical discontinuity, and a homeotropic optically extinct texture. The presence of these defect textures characterizes the mesophase as smectic A. Subsequent cooling leads to the homeotropic areas becoming *schlieren* (see figure 6), and the focal-conic domains becoming broken: both of these textures are characteristic of the formation of a smectic C phase. As the temperature is lowered there is the formation of a third phase, again characterized by the presence of a *schlieren* texture (see

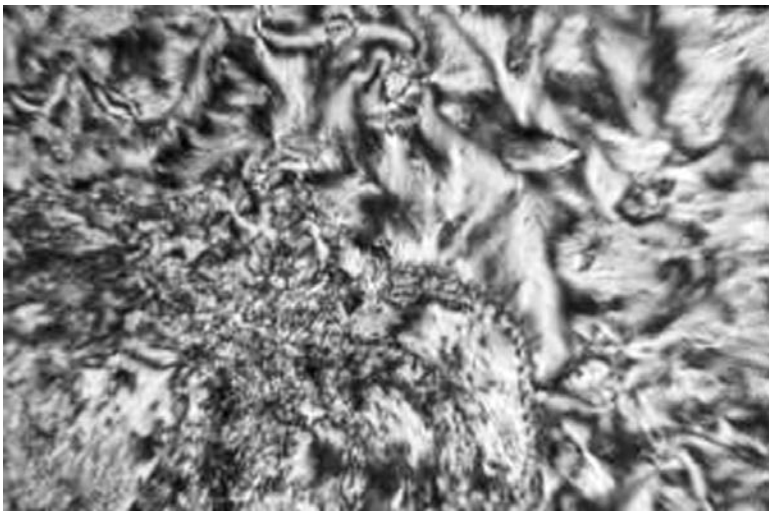

Figure 6. The *schlieren* texture of the smectic C phase of the racemate (× 100).

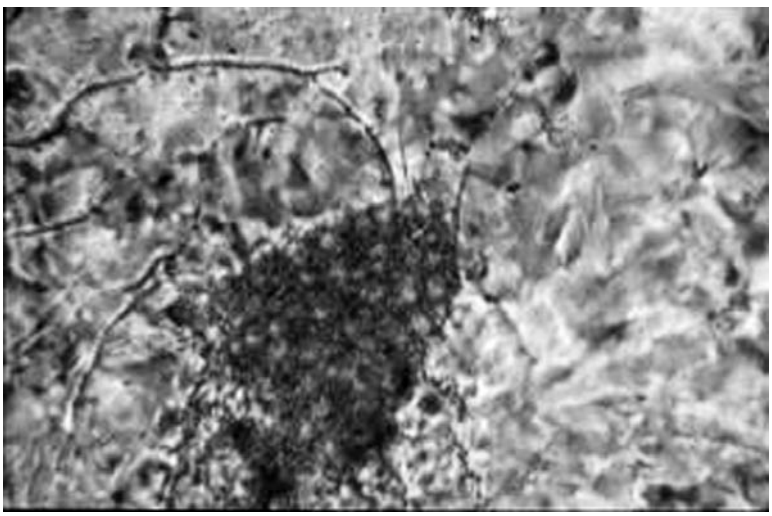

Figure 7. The *schlieren* texture of the anticlinic smectic C (SmC_{alt}) phase of the racemate (× 100).

figure 7), but this time the focal conic domains are not as broken as they were in the smectic C phase. These observations are in keeping with the third phase being an *anticlinic* smectic C_{alt} phase, where the tilt directions of the molecules alternate on passing from one layer to the next, i.e. the tilt direction rotates through an angle of 180° on passing from one layer to the next. Thus the racemate appears to exhibit an SmA, SmC, SmC_{alt} phase sequence, whereas the (S)-enantiomer exhibits a TGB and SmC^*_A sequence.

The effect of increasing the optical purity of the system is to suppress the formation of the smectic A^* and smectic C^* phases to the benefit of the antiferroelectric SmC^* phase and the introduction of a frustrated TGB phase. This clearly demonstrates that the phase transitions and the transition temperatures are chirality dependent. The effects of chirality on the phase transitions are equally clearly demonstrated by calorimetry.

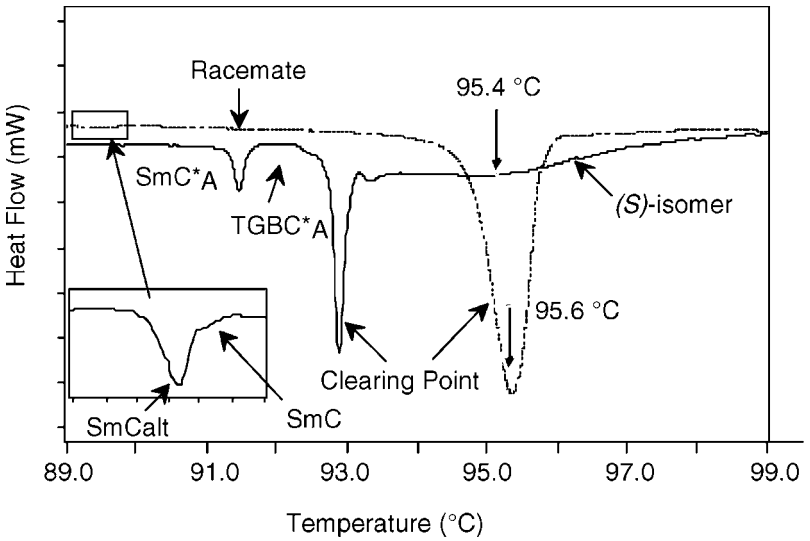

Figure 8. Differential scanning thermograms obtained on cooling for the (S)-enantiomer, **II** (solid lines) and its racemic modification (dotted lines); the scan rate was 2 °C min^{-1}.

3.3. Differential scanning calorimetry

Differential scanning calorimetry, at a variety of scanning rates, was used to investigate the nature of the phase transitions and to determine their associated enthalpy values, which are given in table 1.

Figure 8 shows the cooling scans for both the racemic modification and the (S)-enantiomer. For the racemate (dotted line) the smectic A phase forms first on cooling from the isotropic liquid at 96 °C. On further cooling a smectic C phase is formed at 90.5 °C, but as the transition is second order it is detected only as a baseline step in the DSC. As the temperature is lowered a weak first order transition is found for the smectic C to smectic C_{alt} at 89.2 °C.

The enantiomer, the solid line in figure 8, shows strong pretransitional effects in the isotropic liquid just before the transition to the TGB phase. At a scan rate of 10 °C min^{-1} these effects become more pronounced as shown in figure 9. A distinct depression appears which has a minimum at roughly the same temperature as the smectic A phase is formed from the isotropic liquid for the racemate. Transitional effects in the isotropic liquid are typical for systems that are about to form TGB phases and are associated with entangled or disentangled flux phases, i.e. the amorphous liquid has some long range order associated with it [18]. The transition to the TGB phase is strongly first order, but the associated enthalpy is much lower than that obtained for the clearing point of the racemate. However, the enthalpy for the isotropic liquid to smectic A transition is approximately equal to the sum of the enthalpies associated with the pretransitional effect in the liquid and the isotropic liquid to TGB phase of the enantiomer [3, 4].

3.4. Miscibility studies

A miscibility phase diagram was constructed for binary mixtures of the racemate and the (S)-enantiomer, **II**, thereby giving the phase transition temperatures as a function of optical purity. Binary mixtures were prepared by weighing out each of the components onto a glass slide, heating them until they were in their liquid states, then mixing them with a spatula tip

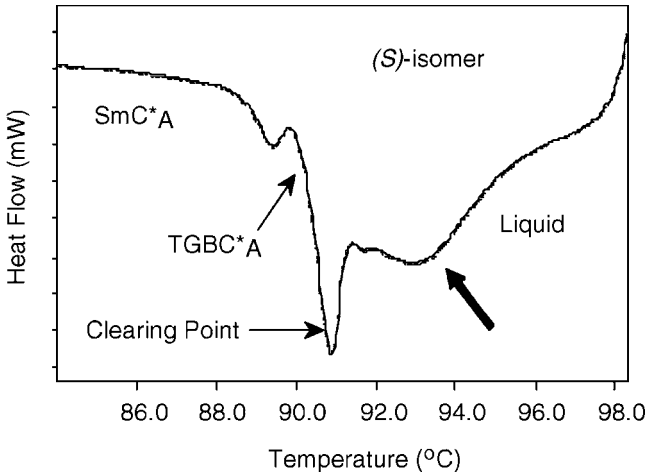

Figure 9. Differential scanning thermogram obtained on cooling for the (S)-enantiomer, **II**; the scan rate was 10 °C min^{-1}.

and placing a cover-slip over the resulting liquid. The transition temperatures for each binary mixture were then determined by thermal polarized light microscopy.

Figure 10 shows the transition temperatures of the various binary mixtures as a function of concentration. It can be seen that as the optical purity is increased the smectic A* and smectic C* phases are suppressed, and the antiferroelectric smectic C* phase becomes relatively stabilized. Part of the way across the phase diagram, at about 75% of the racemate in the mixture, a TGB phase is introduced. The defect textures exhibited by this TGB phase are indicative of it being a TGBA* modification, see figure 11 [3, 4].

It can also be seen from figure 10 that the temperature range of the TGB phase widens considerably when the (S)-enantiomer is in an excess of greater than 50%. Electrical field studies indicate that at this point the nature of the TGB phase changes from TGBA* to $TGBC_A^*$. However, no phase transition from one TGB phase to the other could be detected in the phase diagram, which might be due to the sharpness of the cross-over from one modification to the other.

In the range of 30 to 50% of the racemate in the binary mixtures (see cross-hatched area in figure 10), the smectic A* and smectic C* phases exhibited homeotropic textures and as a consequence were hard to distinguish from one another. In the absence of alternative techniques for investigation we can postulate two possibilities for the phase behaviour in this region of the diagram. Either there is a boundary line between the smectic A* and smectic C_A^* phases (dotted line on the right-hand boundary of the cross-hatched region), which arises from thermodynamic considerations that exclude the appearance of a smectic A* phase between the $TGBC_A^*$ and smectic C_A^* phases, or, if the two data points on the lower portion of the hatched area correspond to real phase transitions, rather than say to a shortening of the helical pitch, then we can speculate that the presence of the smectic A* phase is related to some form of re-entrancy. Detailed investigations of this region of the phase diagram are currently being undertaken using a variety of techniques, the results of these studies will be reported in the near future.

3.5. Electrical field studies

The spontaneous polarization in the antiferroelectric phase of compound **II** was determined, as a function of the reduced temperature from the Curie point, using the triangular wave techniques

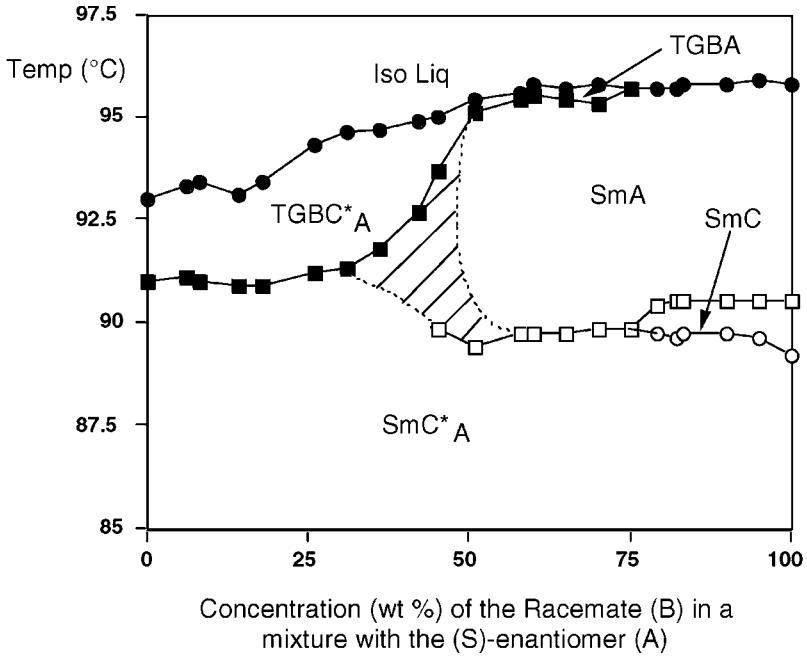

Figure 10. Binary phase diagram, as a function of concentration (wt%) and temperature (°C), between the (S)-enantiomer, **II**, A and its racemate, B.

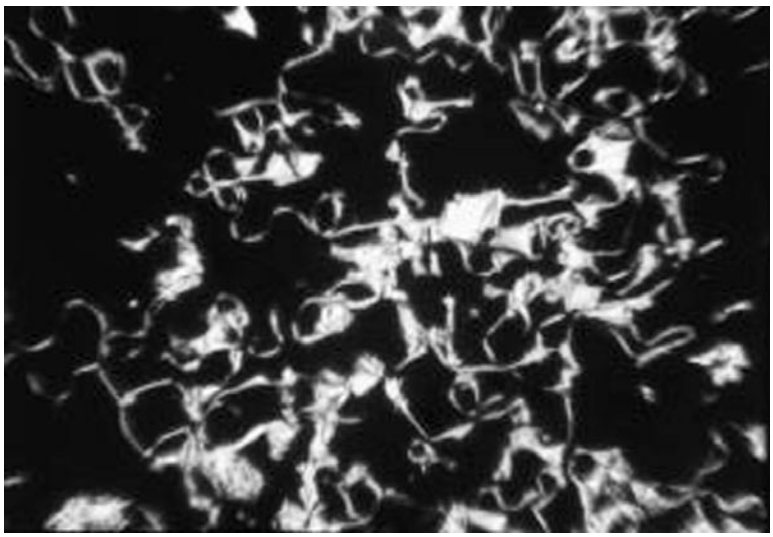

Figure 11. The filament texture at the TGBA* transition for a mixture of the racemate (70%) and the (S)-enantiomer (30%) (×100).

described earlier. It should be noted that the measurement of the spontaneous polarization in an antiferroelectric phase is an artefact of the current flow reversal for switching between the two ferroelectric fully switched states, i.e. it is the sum over the double hysteresis loop. Figure 12 shows that the polarization rises from a low value at the Curie point to give a saturated value

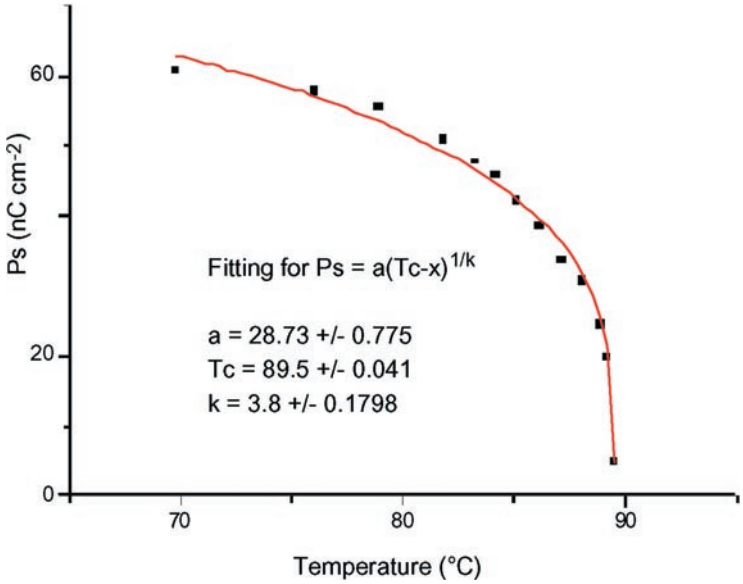

Figure 12. The spontaneous polarization (nC cm^{-2}) measured as a function of temperature for compound **II**.

of approximately 60 nC cm^{-2} at a reduced temperature of 20 °C. Thus for an antiferroelectric material with a structure based on the 1-methylheptyl moiety the spontaneous polarization is relatively low.

Examination of the current flow as a function of temperature and time, see figure 13, shows that as the material is switched from one stable ferroelectric state to the other two separate events occur which correspond to switching from one ferroelectric state to the antiferroelectric state and on to the other ferroelectric state. As the temperature is reduced so the antiferroelectric state becomes more stable, which is probably reflected in a higher viscosity. At the transition to the TGB phase there is no appreciable change in the switching process indicating that the phase formed from the TGB phase on cooling is indeed antiferroelectric, confirming the observations made from the miscibility studies, i.e. that compound **II** does not exhibit either a smectic A* or smectic C* phase that correspond to the achiral phases of the racemate.

During the switching processes samples of compound **II** were observed in the microscope. Figures 14–16 show remarkable behaviour at the TGB to antiferroelectric phase transition. In the three plates the antiferroelectric phase is on the right-hand side and the TGB phase on the left. As the field is reversed the dark stable ferroelectric state in figure 14 passes through an intermediary stable state corresponding to the antiferroelectric phase, figure 15, before reaching the second stable light ferroelectric state shown in figure 16. The TGB phase can also be seen to follow the same switching pattern indicating that it too has a bulk antiferroelectric structure.

It is also interesting to examine more closely the complicated events that appear to take place during the switching of the TGB phase. On cooling from the isotropic liquid, the homogeneous alignment layer of the cell causes the TGB phase to form with its heli-axis approximately perpendicular to the glass substrates. Upon the application of an applied electric field the helical structure becomes distorted, and during this process the defects (screw dislocations) associated with grain boundaries of the TGB phase apparently anneal and the

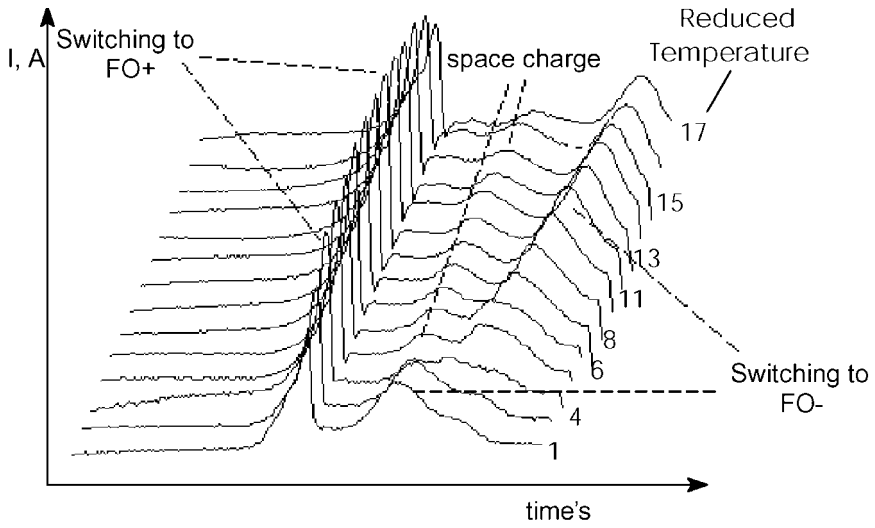

Figure 13. The time (s) current trace as a function of the reduced temperature ($\Delta T = T - T_C$) from the TGB to antiferroelectric phase transition using the triangular wave method. The movement of space charge is clearly seen and isolated by this technique.

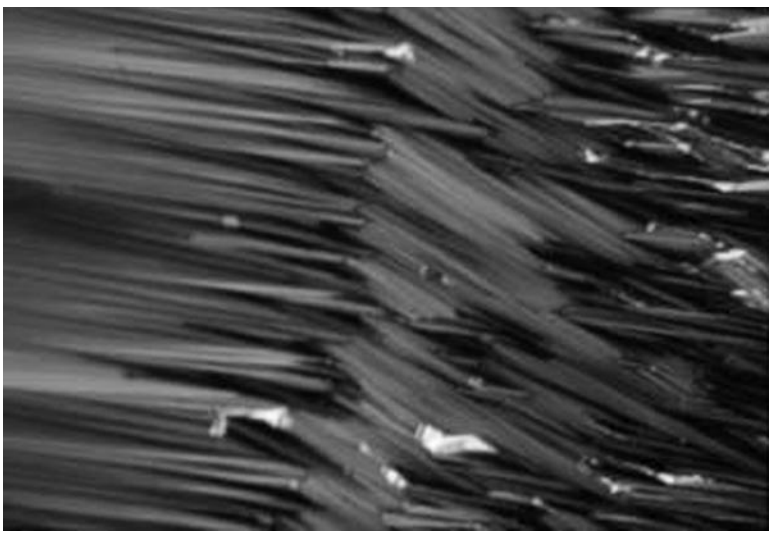

Figure 14. The switched ferroelectric (right-hand side) and TGB states (left-hand side) of compound **II**, ± 20 V μm^{-1}, at 0.2 MHz ($\times$ 100).

helical structure partially unwinds. The degree to which the system becomes unwound seems to depend on variations in cell thickness and surface pinning defects etc. A form of balance is reached between the unwinding of the TGB structure and the degree to which the system is switched into an antiferroelectric state. In the antiferroelectric state a helical macrostructure would be expected to be formed parallel to the cell substrates and perpendicular to the heli-axis of the TGB phase. However, coupling of the local spontaneous polarization to the applied electric field can induce a further transformation to an unwound switched ferroelectric state. Variations caused by thickness variations and surface pinning effects lead to the antiferroelectric

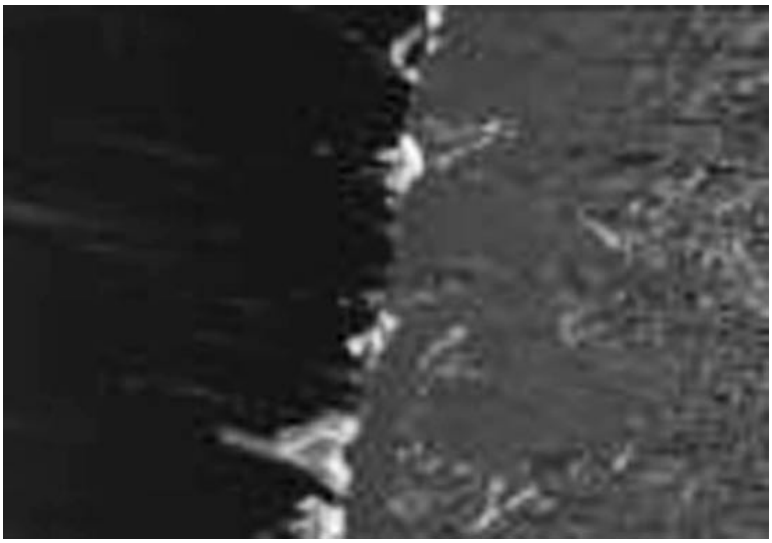

Figure 15. The antiferroelectric (right-hand side) and TGB states (left-hand side) of compound **II**, ± 20 V μm^{-1}, at 0.2 MHz ($\times$ 100).

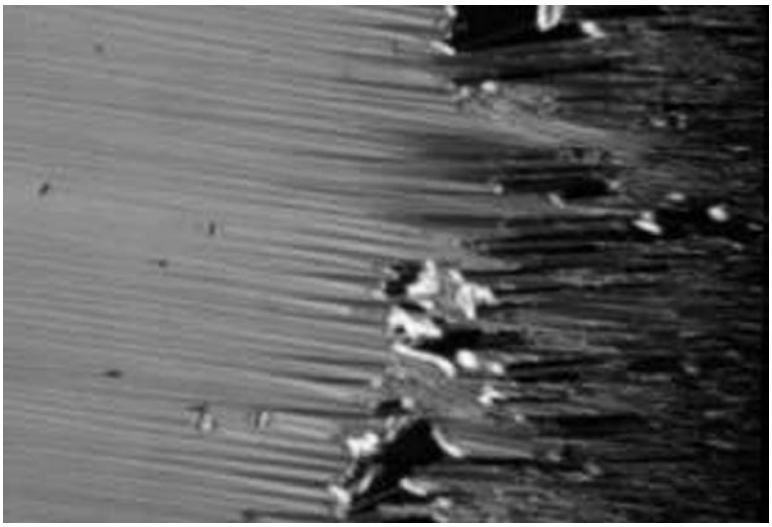

Figure 16. The second switched ferroelectric (right-hand side) and TGB states (left-hand side) of compound **II**, ± 20 V μm^{-1}, at 0.2 MHz ($\times$ 100).

state possessing some regions where a helical macrostructure forms in the plane of the cell and other regions that are completely unwound. Increasing the applied electric field totally unwinds the structure and the molecules reorganize to give a stable switched ferroelectric state.

The results obtained from dielectric spectroscopy studies are exemplified in figure 17(a) and (b). The plot in 17(a) shows measurements taken on heating from 86 to 93 °C, and the plot shown in 17(b) was generated on cooling from 93 to 86 °C. Between 88 and 91 °C broadening of the modes occurs indicating the presence of a phase transition that corresponds to the antiferroelectric to twist grain boundary phase change. It is likely that the broadening is due to a soft-mode-like absorption associated with the occurrence of tilt-angle fluctuations in the

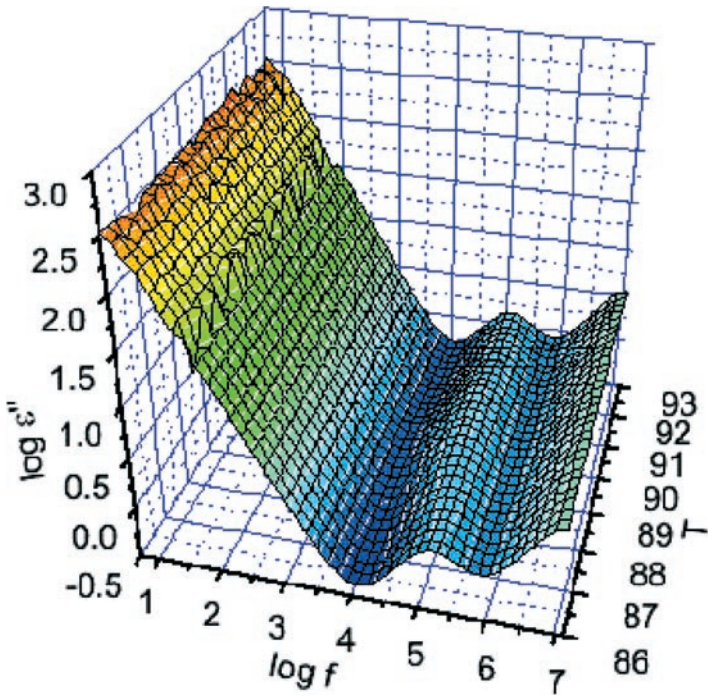

(a)

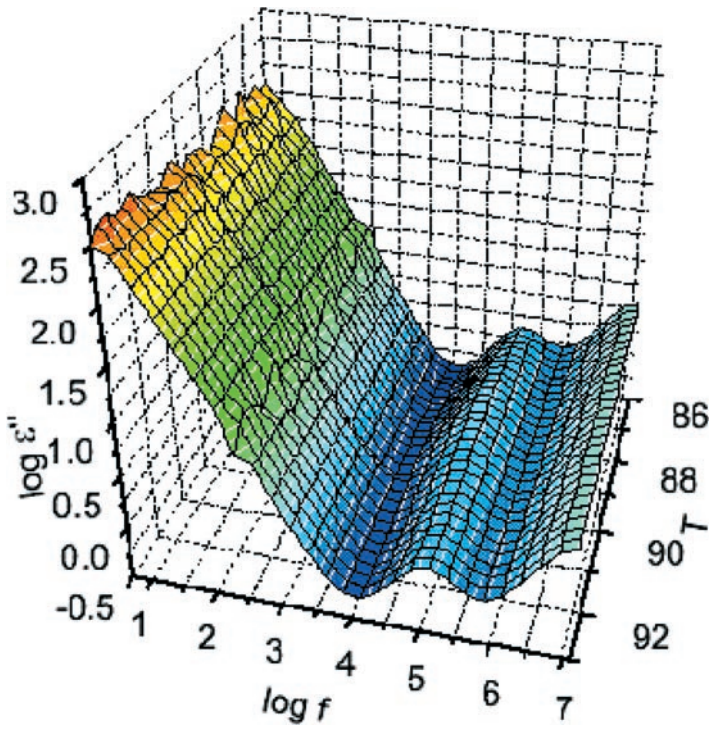

(b)

Figure 17. (a) Dielectric spectroscopy measurements on the (S)-enantiomer, **II**, taken on heating from 86 to 93 °C, and (b) results obtained on cooling from 93 to 86 °C.

SmC^*_A and TGB phases. The fact that this mode does not change *at all*, except at the point of the phase transition, indicates the structures of the two phases are very similar and therefore, like the antiferroelectric phase, the TGB phase has a local alternating tilt (anticlinic) structure. We stress that we have not yet obtained any firm evidence to confirm this mode is really related to the tilt angle fluctuations; nevertheless this hypothesis still remains the most likely explanation.

4. Discussion

We have shown via a number of techniques that (S)-1-methylheptyl 2-[4-(4′-dodecyloxybenzoyloxy)phenyl] pyrimidine-5-carboxylate, **II**, exhibits TGB and antiferroelectric smectic C^*_A phases whereas its racemic modification possesses smectic A, smectic C and smectic C_{alt} phases. The character and structure of the TGB phase is interesting because the phase shows three state switching and novel defect textures which indicate that it has a local antiferroelectric structure. This means that the mesophase will be composed of a layered structure that will be punctuated with a lattice of screw dislocations. The screw dislocations will induce a twist of sheets or blocks of the phase about an axis parallel to the layers of the phase. Between the screw dislocations the molecules will be tilted in layers with the tilt directions rotating through 180° on passing from one layer to the next, as in an antiferroelectric phase. A schematic diagram of the proposed structure of this new and interesting state of matter is shown in figure 18.

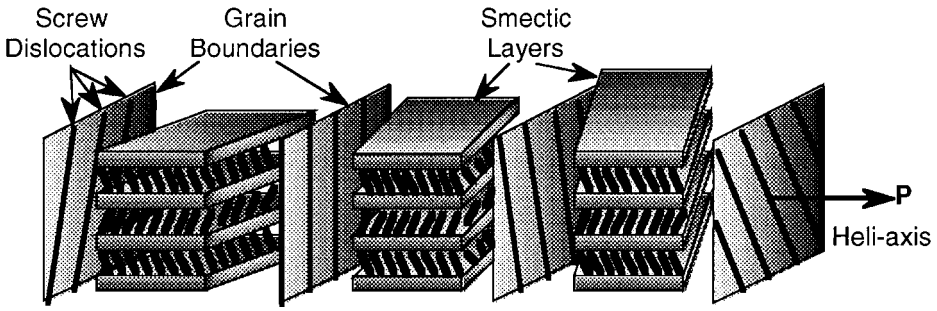

Figure 18. A schematic diagram of the proposed structure of the antiferroelectric $TGBC^*_A$ phase.

This model has two possible variations, one where the interlayer twist of the normal antiferroelectric phase is expelled to the dislocations in the TGB phase, and one where there is a twist perpendicular to the layers and to the in-plane heli-axis of the TGB phase. For the situation where the interlayer twist is expelled to the screw dislocations, the polarization vector can lie either perpendicular or parallel to the heli-axis. The way in which the helix of the TGB phase reorients in the electrical field studies suggests that the polarization vector is probably perpendicular to the in-plane twist, much as it is in the TGBC phase [19, 20]. Finally we note that the commensurability/incommensurability of the in-plane twist cannot be gauged from these studies. Further investigations using x-ray diffraction will be able to elucidate these possibilities.

5. Conclusion

We have comprehensively demonstrated that (S)-1-methylheptyl 2-[4-(4′-dodecyloxybenzoyloxy)phenyl] pyrimidine-5-carboxylate exhibits a novel TGB—antiferroelectric smectic C^*_A phase. This phase is an analogue of the Abrikosov flux phase found in

superconductors. This result represents the addition of a new frustrated state of matter to the family of twist grain boundary phases.

Acknowledgments

We would like to thank the University of Hull Overseas Research Student Scheme, the Department of Chemistry, University of Hull, the EU TMR programme (Optical Research of Chiral Systems ORCHIS) and DERA for financial support.

References

[1] de Gennes P 1972 *Solid State Commun.* **10** 753
[2] Renn S R and Lubensky T C 1988 *Phys. Rev.* A **38** 2132
[3] Goodby J W, Waugh M A, Stein S M, Chin E, Pindak R and Patel J S 1989 *Nature* **337** 449
[4] Goodby J W, Waugh M A, Stein S M, Chin E, Pindak R and Patel J S 1989 *J. Am. Chem. Soc.* **111** 8119
[5] Slaney A J and Goodby J W 1991 *J. Mater. Chem.* **1** 5
[6] Slaney A J and Goodby J W 1991 *Liq. Cryst.* **9** 849
[7] Bouchta A, Nguyen H T, Achard M F, Hordouin F, Destrade C, Tweig R J, Maaroufi A and Isaert N 1992 *Liq. Cryst.* **12** 575
[8] Strajer G, Pindak R, Waugh M A, Goodby J W and Patel J S 1990 *Phys. Rev. Lett.* **64** 1545
[9] Navailles L, Barois P and Nguyen H T 1993 *Phys. Rev. Lett.* **71** 545
Navailles L, Pindak R, Barois P and Nguyen H T 1995 *Phys. Rev. Lett.* **74** 5224
Navailles L, Barois P and Nguyen H T 1994 *Phys. Rev. Lett.* **72** 1300
[10] Takatoh K, Lamb A G M and Goodby J W, unpublished results.
[11] Pramod P A, Pratibha R and Madhusudana N V 1997 *Current Sci.* **73** 761
[12] Goodby J W, Nishiyama I, Slaney A J, Booth C J and Toyne K J 1993 *Liq. Cryst.* **14** 37
[13] Goodby J W, Hird M, Lewis R A and Toyne K J 1996 *J. Chem. Soc. Chem. Commun.* **27** 19
[14] Miyaura N,Yanmada K and Suzuki A 1979 *Tetrahedr. Lett.* 3437
Miyaura N and Suzuki A 1979 *J. Chem. Soc. Chem. Commun.* 866
[15] Mitsunobu O 1981 *Synthesis* 1
[16] Priest R C (ed) 1988 *CRC Handbook of Physics and Chemistry* 68th edn (Boca Raton, FL: Chemical Rubber Company)
[17] Gilli J M and Kamayé 1992 *Liq. Cryst.* **12** 545
[18] Goodby J W, Dunmur D A and Collings P J 1995 *Liq. Cryst.* **19** 703
[19] Renn S R and Lubensky T C 1991 *Mol. Cryst. Liq. Cryst.* **209** 349
Renn S R 1992 *Phys. Rev.* A **45** 953
[20] Petit M, Barois P and Nguyen H T 1996 *Europhys. Lett.* **36** 185